Biointerface Research in Applied Chemistry
Open-Access Journal (ISSN: 2069-5837)

Article
Volume 14, Issue 2, 2024, 44
https://doi.org/10.33263/BRIAC142.044

Improving the Fluorescence of Carbon Dots Through Boron and Silver Doping: A Single-Step Microwave Synthesis Approach

Yanika Sakboriboon [1], Jongjit Chalitangkoon [1], Pathavuth Monvisade [1,*]

[1] Polymer Synthesis and Functional Materials Research Unit, Department of Chemistry, School of Science, King Mongkut's Institute of Technology Ladkrabang, Chalongkrung Road, Ladkrabang, Bangkok 10520, Thailand
* Correspondence: pathavuth.mo@kmitl.ac.th;

Scopus Author ID 18133833400
Received: 28.03.2023; Accepted: 28.05.2023; Published: 4.02.2024

Abstract: Carbon dots (CDs) are a promising type of fluorophore with numerous advantages such as low toxicity, biocompatibility, good photostability, and ease of synthesis. However, their low quantum yields (QYs) have limited their applicability in many fields. Researchers have turned to doping CDs with nonmetallic and metallic atoms to address this issue. In this study, we synthesized citric acid/urea-based CDs doped with boron and/or silver atoms in a single step using microwave irradiation. Transmission electron microscopy (TEM) and Fourier transform infrared spectroscopy (FTIR) were used to characterize the CDs. In contrast, UV-visible (UV-Vis) and fluorescence spectroscopy were used to examine their optical properties. We discovered that all synthesized CDs were transparent to visible light and emitted blue fluorescence when exposed to UV light. Our fluorescence analysis revealed that doping with both boron and silver atoms led to higher fluorescence compared to doping with only one of the atoms. Specifically, the quantum yields (QYs) of silver/boron-doped CDs were 26%, which is higher than those of silver-doped CDs (19%), boron-doped CDs (9%), and undoped CDs (6%). These findings suggest that the silver/boron-doped CDs produced using our simple method could be promising materials for sensors and biomedical applications.

Keywords: carbon dots; doping with heteroatom; doping with metal atom; quantum yields.

1. Introduction

Carbon dots (CDs) are a type of fluorescent nanoparticle that was discovered in 2004 by Xu's group while using electrophoresis to purify single-walled carbon nanotubes [1]. Generally, CDs have quasi-spherical shapes with sizes less than 10 nm and display multicolor emission [2-4]. Various methods have been used to synthesize CDs, such as microwave heating [5], hydrothermal synthesis [6], arc discharge [7], laser ablation [8] and electrochemical synthesis [9]. The precursor of CDs is critical to their fluorescence behavior due to the diverse chemical structures of the core and surface that arise from various carbon sources [10,11]. Chemicals and daily foods such as citric acid [12], glycerol [13], urea [14], coffee [15], pumpkin [16], orange juice [17], and others have been used as CD sources. CDs have gained popularity due to their ease of synthesis, low toxicity, excitation wavelength dependence, and ease of surface passivation [18]. These unique properties make them attractive candidates for sensing, bioimaging, drug delivery, and other fields [19]. However, their low quantum yields

(QYs) have hindered their widespread use. Researchers have been looking into ways to improve their QYs and functionality to address this issue.

Doping, which involves introducing atomic impurities into the structure of carbon dots (CDs), is a commonly used method for improving their properties. Doping can change CDs' electronic structure, nanostructure, and chemical composition by overlapping the atomic orbitals of heteroatoms and carbon atoms [20, 21]. Several heteroatoms, such as B, N, F, P, S, and others, are now widely used as doping agents by researchers to improve CDs' QYs, solubility, and physicochemical properties [22-24]. Kiem *et al*., for example, synthesized N-doped CDs using glucose and urea as precursors in a hydrothermal method, resulting in a significant improvement in fluorescence emission properties with QYs of 9.6% compared to pure glucose, and the resulting CDs were used as a chemical sensor for detecting carcinogenic, hemotoxic, and genotoxic chromium (VI) [25]. To enhance the quantum yields (QYs) of carbon dots (CDs), N and B dopings are frequently employed as heteroatoms. These dopings modify the conduction/valence band position of CDs by incorporating neighboring elements in the periodic table, which results in improved fluorescence characteristics [26-29]. In their study, Jiali *et al*. utilized a solvothermal method to produce N, B-doped carbon dots (CDs) by using p-phenylenediamine and boric acid as precursors. The resulting CDs demonstrated photoluminescence with a high quantum yield (QY) of 17%. The N, B-doped CDs proved to be promising nanoprobes for detecting Cu^{2+} and Co^{2+} due to their high sensitivity and selectivity [30]. The distinctive electronic structure of Co-doped CDs arises from the combined effect of the heteroatoms, which results in higher QYs compared to CDs doped with a single atom [31].

The distinctive physicochemical characteristics of metal nanoparticles have made them a subject of great interest in various fields, including photovoltaics, catalysis, and biology [32]. Among various metals, less toxic and eco-friendly ones such as Ag, Au, Ga, and La have been explored as dopants for CDs [33]. Wang *et al*. conducted a study in which they used hydrothermal methods to synthesize CDs co-doped with Ag and N. They employed precursors such as silver nitrate, citric acid, and ammonia solution to achieve this. The resulting CDs displayed remarkable photoluminescence with QYs of 35% and effective antimicrobial activity against both Gram-negative bacteria (Escherichia coli) and Gram-positive bacteria (Staphylococcus aureus) [34]. Metal doping is considered superior to heteroatom doping when it comes to enhancing the fluorescence properties of CDs. This is because metals function as electron donors, have more unoccupied orbitals, and have a larger atomic radius. As a result, they bring about changes in charge density and charge transition forms between metal ions and graphene matrix, which ultimately leads to improved fluorescence properties of CDs [35-38].

In our study, we present a straightforward and low-toxicity approach to enhance the QYs of CDs by doping them with nonmetallic and/or metallic atoms. We synthesized boron and/or silver-doped citric acid/urea-based CDs using citric acid, urea, borax, and silver nitrate as precursors through a single-step microwave irradiation method. The synthesized CDs exhibit pH-dependent fluorescence, making them suitable for use as pH sensors, and we investigated the mechanisms underlying their pH sensitivity. Our findings indicate that the CDs doped with silver and/or boron using this simple method have the potential for use in biomedical applications and as sensor materials.

2. Materials and Methods

2.1. Materials.

Citric acid, urea, and sodium tetraborate decahydrate were purchased from Carlo Erba. Silver nitrate was purchased from Fisher Chemical. All the chemicals were analytical grade and were used without further purification.

2.2. Synthesis of carbon dots.

Citric acid/urea-based CDs and citric acid/urea-based carbon dots doped with silver were synthesized by cojoining two previously reported methods [39,40] with some modifications. In the first step, 3 g each of citric acid and urea were dissolved in 100 mL deionized water and stirred for 30 min. Then, 15 mL of distilled water or 1 mM $AgNO_3$ was added to 20 mL of the solution. The resultant mixture was stirred for 15 minutes, following which it was placed in an 800W domestic microwave oven for 3 min. The crude product was dissolved in 20 mL of deionized water and filtered through a 0.2 µm syringe filter. Finally, the product was dried in an oven at 60°C for two days. The samples were labeled CU-CDs for undoped carbon dots and CU/Ag-CDs for silver-doped CDs.

Boron-doped CDs were synthesized using the same process, with minor changes. Briefly, 3 g borax was added to the 100 mL citric/urea solution. After that, the following steps were carried out as mentioned above. The samples were labeled BCU-CDs for boron-doped carbon dots and BCU/Ag-CDs for boron/silver-doped carbon dots.

2.3. Attenuated Total Reflection Fourier Transform Infrared Spectroscopy (ATR-FTIR).

The ATR-FTIR spectrometer (IRTracer-100, Shimadzu, Japan) was used to examine the functional groups present on the surface of carbon dots. The scanning range for the samples was from 500 to 4000 cm^{-1}.

2.4. X-ray photoelectron spectroscopy (XPS).

An X-ray photoelectron spectrometer was used to characterize the element composition in the structure of carbon dots. (Shimadzu, Kratos Axis ultra DLD, Japan).

2.5. UV-Visible Spectroscopy (UV-Vis).

The characteristic absorbance of carbon dots was recorded using a UV-vis spectrophotometer (Lab Tech, BlueStar B, China). The samples were scanned over a range of 200-500 nm.

2.6. Fluorescent spectroscopy.

Carbon dots' fluorescence spectra and optimum excitation-emission wavelength were characterized using a fluorescence spectrofluorometer (RF-6000, Shimadzu, Japan).

2.7. Quantum yield measurement.

The quantum yield (Ø) for each of the CDs was determined by utilizing the following formula, with quinine sulfate in 0.1 M H_2SO_4 serving as the reference.

$$\phi = \phi_s \left[\frac{F \times A_s \times n^2 \times D}{F_s \times A \times n^2{}_s \times D_s} \right]$$

where Ø is the quantum yield, $Ø_s$ is the quantum yield of the standard sample, F is the peak area of the unknown sample, F_s is the peak area of the standard sample, A is the absorbance of the unknown sample at the excitation wavelength, A_s is the absorbance of the standard sample at the excitation wavelength, η is the refractive index of the unknown sample, η_s is the refractive index of the unknown sample, D is the dilution factor of the unknown sample, and D_s is the dilution factor of the standard sample.

2.8. Transmission electron microscopy (TEM).

The morphology and size distribution of CDs were characterized using a transmission electron microscope (HRTEM, JEM-2100Plus, JEOL, USA) with lanthanum hexaborate (LaB_6) as the electron source and the accelerating voltage 200 kV.

2.9. pH-responsive carbon dots

The pH values were modified to evaluate the impact of pH on the emission intensity of CDs while the excitation was held constant at 350 nm. A standard experiment involved combining 1 mL of a 1%w/v CDs solution with buffer pHs ranging from 2 to 12. Additionally, a digital camera captured visual images under daylight and UV light. The emission intensity was characterized using a spectrofluorometer [41].

3. Results and Discussion

3.1. Synthesis of carbon dots.

The carbon dots with a citric acid/urea base were synthesized using domestic microwave irradiation in a one-step process. Citric acid was employed as the carbon source, while urea, borax, and silver nitrate were utilized as the sources of nitrogen, boron, and metal, respectively.

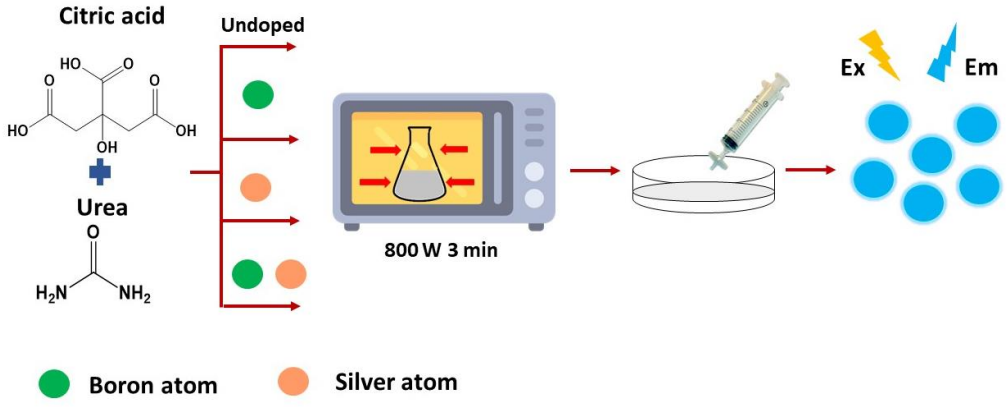

Figure 1. Carbon dots synthetic scheme.

The synthesis steps are depicted in Figure 1. The fluorescence intensity of the CDs increased with microwave irradiation time, reaching a maximum of 3 minutes, as shown in Figure 2. However, when the microwave irradiation time increased to 4 min, the fluorescence

intensity of CDs decreased because the surface structure of CDs was destroyed, leading to a decrease in emission intensity [42].

Furthermore, at 4 min of microwave irradiation, the emission wavelength shifted to a higher wavelength, indicating that CDs contain a mixture of green and blue colors. Based on the fluorescence spectra, it can be observed that CDs synthesized at 3 min exhibited the highest emission due to the synergistic effect of the surface and carbogenic core [43]. As mentioned previously, the optimal time to synthesize all CDs was found to be 3 min.

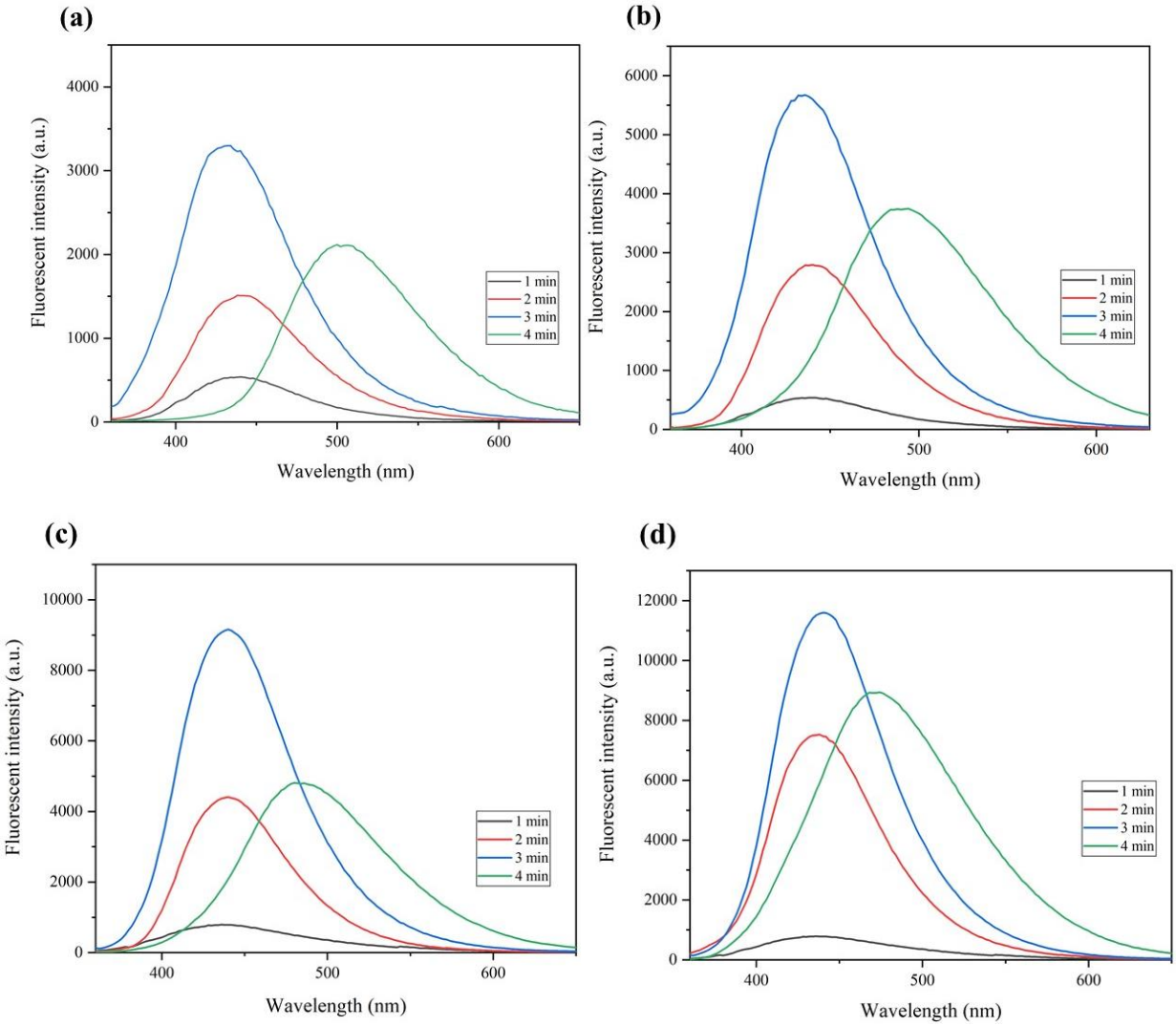

Figure 2. Microwave pyrolysis time of **(a)** CU-CDs; **(b)** CU/Ag-CDs; **(c)** BCU-CDs; **(d)** BCU/Ag-CDs.

3.2. ATR-FTIR spectroscopy.

To determine the functional groups, present on the surface of the CDs, the FTIR spectra presented in Figure 3 were examined. All synthesized CDs demonstrated peaks at 3392-3197, 2980, 1666, and 1620 cm−1, corresponding to the stretching vibration of O-H/N-H, C=C, C-H, and C=O, respectively. The presence of nitrogen atoms in the CDs structure was indicated by the stretching of C-N and N-H bonds at 1307 cm^{-1} and 3405-3500 cm^{-1}. Additionally, the peaks at 1382 and 1031 cm^{-1} were attributed to the B-O and B-O-C vibrations, respectively, indicating the successful doping of boron atoms into BCU-CDs and BCU/Ag-CDs. However, the vibration of silver atoms was not noticeable due to the small quantity added, and there was

an overlap of the peak. The results indicated that the CDs contain plenty of carboxyl and hydroxyl groups, resulting in their hydrophilic behavior [44,45].

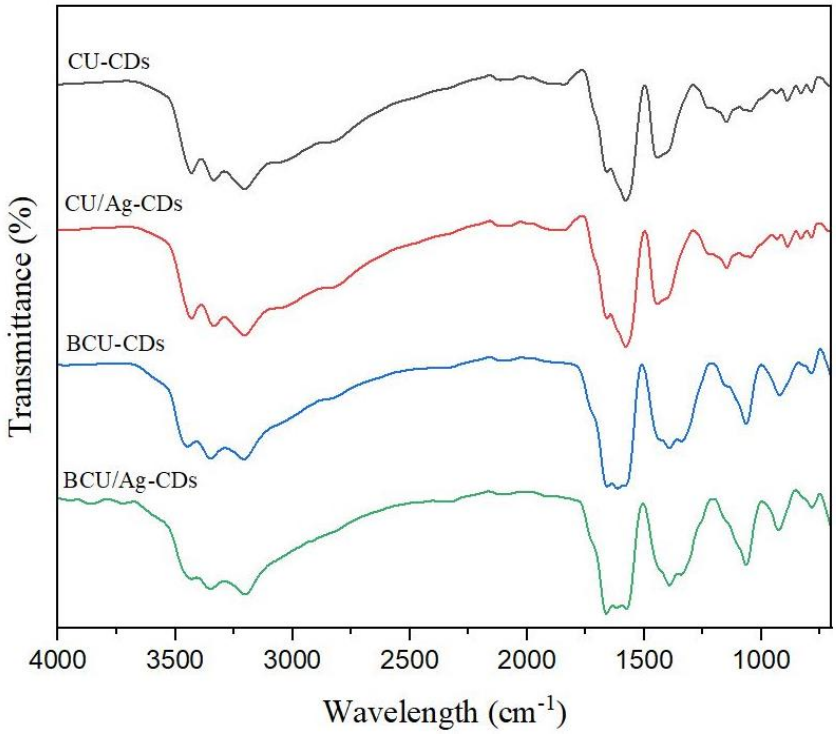

Figure 3. FTIR-spectrum of each carbon dot.

3.3. X-ray photoelectron spectroscopy.

To verify the surface composition and the doping of nitrogen, boron, and silver atoms in the carbon dots (CDs) structure, X-ray photoelectron spectroscopy (XPS) was used to analyze BCU/Ag-CDs. The XPS survey spectra displayed in Figure 4a exhibited characteristic peaks, including O1s (530.00 eV), N1s (397.00 eV), C1s (283.00 eV), B1s (190.00 eV), and Ag3d (367.00 eV).

The C1s spectrum in Figure 4b showed characteristic peaks corresponding to C-C (284.86 eV), C=O (286.05 eV), C-N (286.85 eV), and C-O (288.75 eV), while the N1s spectrum in Figure 4c revealed peaks corresponding to C=N-C (399.15 eV), N-(C)3 (399.85 eV), and N-H (401.25 eV). The O1s spectrum in Figure 4d displayed peaks that can be assigned to C=O (531.65 eV) and C-O (532.65 eV). The high-resolution B1s spectrum in Figure 4e showed peaks attributed to B-C (192.49 eV) and B-O (193.19 eV), while the high-resolution Ag3d spectrum in Figure 4f showed peaks corresponding to Ag (367.35 eV) and Ag_2O (368.25 eV) in $Ag3d_{3/2}$ (372.95 eV) and $Ag3d_{5/2}$ (373.65 eV). The FTIR and XPS spectra results suggest that nitrogen, boron, and silver atoms were successfully doped into BCU/Ag-CDs.

3.3. UV-Vis spectroscopy.

The UV-Vis spectra of the CDs are displayed in Figure 4 and indicate two separate bands. The first band, located at approximately 200 nm, can be attributed to the π-π* transition of -C=C- and -C-C- bonds in the sp^2 hybridized graphitic core. The second band, located around 300 nm, corresponds to the n-π* transition of -C=O, C-N, or -C-OH bonds in the sp^3 hybridized area of the surface carboxyl (-COOH) or amine ($-NH_2$) groups of the CDs [52]. When an

electron is excited to higher energy levels and subsequently returns to the ground state, releasing photon energy, fluorescence occurs [53].

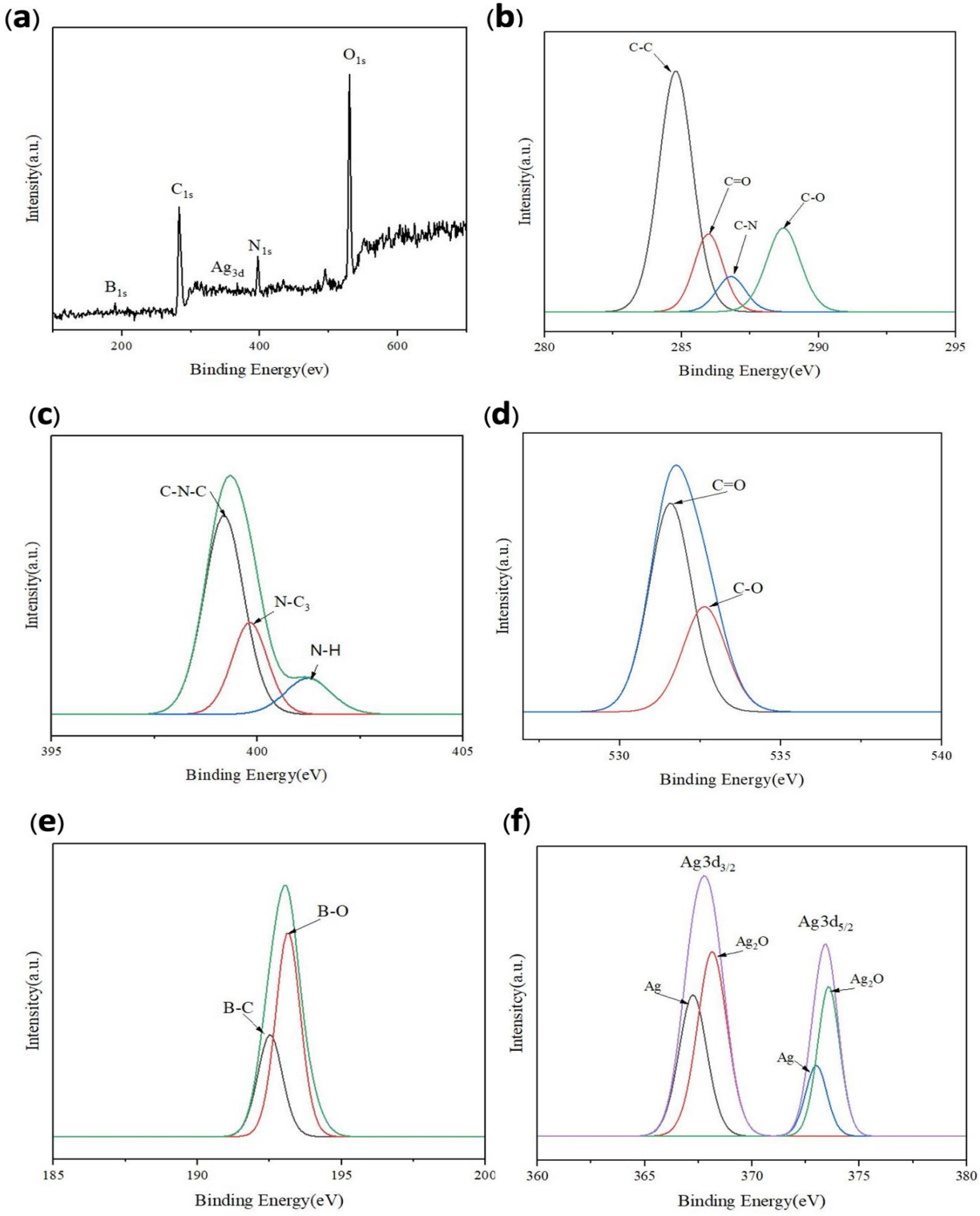

Figure 4. XPS analysis of BCU/Ag-CDs at high resolution, including survey spectra **(a)** and detailed spectra of C1s **(b),** N1s **(c),** O1s **(d),** B1s **(e),** and Ag3d **(f)** orbitals.

Moreover, it can be observed that BCU/Ag-CDs exhibit the highest absorbance intensity in both the π-π* and n-π* transition regions. The doping of electron-rich atoms (boron and silver) into the carbon network results in the transfer of more electrons to the π system, increasing the absorbance intensity [54].

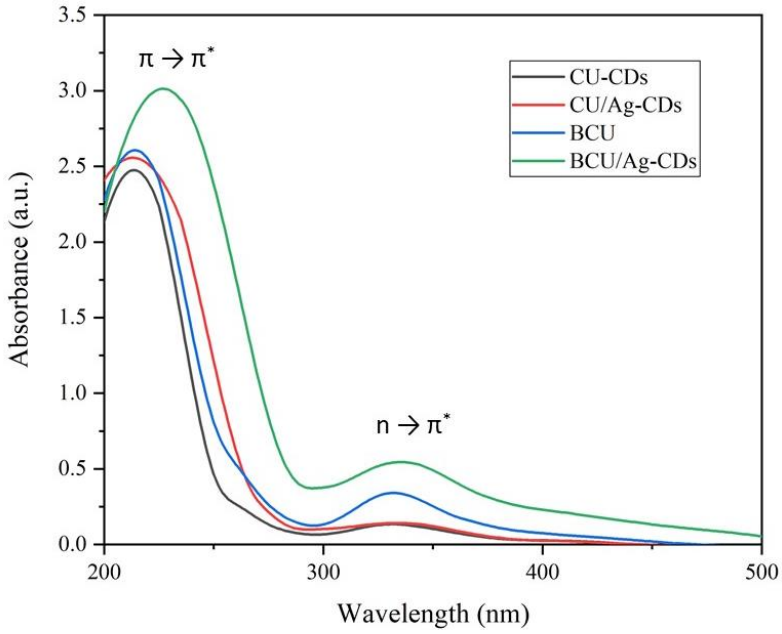

Figure 4. UV-Vis spectra of each CDs.

3.4. Fluorescent spectroscopy

The optimum excitation-emission wavelength and quantum yield of each CD were characterized using a fluorescence spectrometer. The results demonstrated that each CD had a different excitation wavelength to achieve maximum emission, as shown in Figure 5.

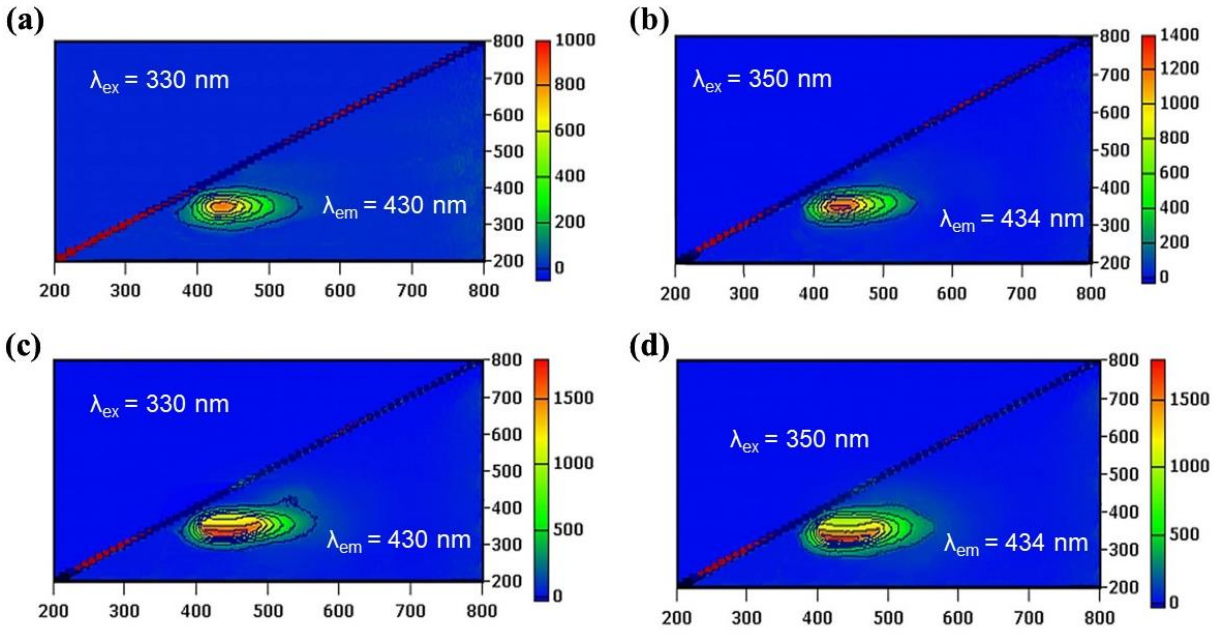

Figure 5. 3D emission-excitation intensity spectra (excitation (y-axis), emission (x-axis)) of **(a)** CU-CDs; **(b)** CU/Ag-CDs; **(c)** BCU-CDs; **(d)** BCU/Ag-CDs.

The quantum yields (QYs) of the CDs were determined using quinine sulfate as a reference in the study. According to the findings, the QYs of undoped CDs was 6%., silver-doped CDs (CU/Ag-CDs) was 9%, boron-doped CDs (BCU -CDs) was 19%, and silver/boron-doped CDs (BCU/Ag-CDs) was 26%. Figure 6 depicts the fluorescent spectra of CDs. The results demonstrated that the BCU/Ag-CDs had the highest intensity compared to the other

CDs, corresponding to their QYs. These results implied that the effect of doping CDs with a heteroatom (boron atom) and metal atom (silver atom) caused a synergistic effect, leading to high QYs [55]. Under visible light, all of the synthesized CDs were transparent, but under UV light, they fluoresced blue, as depicted in Figure 6 inset. Therefore, BCU/Ag-CDs with the highest fluorescence were selected for further experiments.

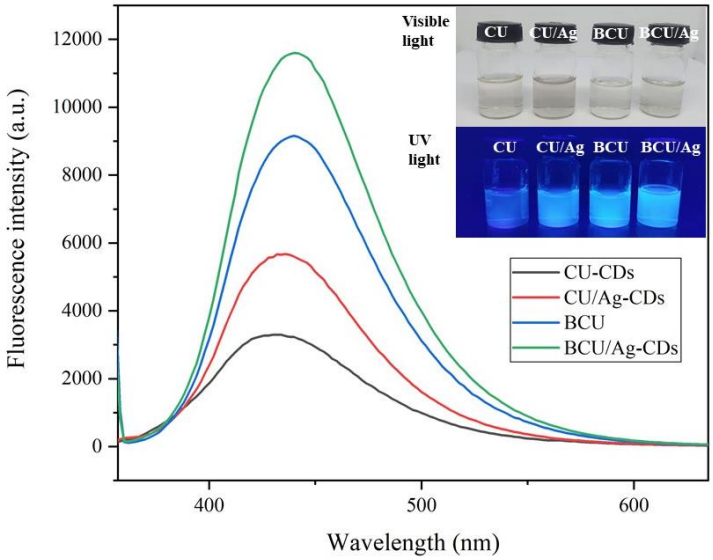

Figure 6. Fluorescent spectra of CDs.

3.5. Transmission electron microscopy (TEM)

The morphology and size distribution of the CDs were examined using transmission electron microscopy (TEM). The TEM image in Figure 7a illustrates that BCU/Ag-CDs were nearly spherical and well-dispersed with an average diameter of 5.9 ± 1 nm. To validate the crystalline nature of the CDs, high-resolution transmission electron microscopy (HRTEM) was employed. The interplanar spacing was measured to be 0.22 nm in Figure 7b, which is equivalent to 100 lattice planes of graphitic carbon. This finding confirms the crystalline nature of BCU/Ag-CDs [56].

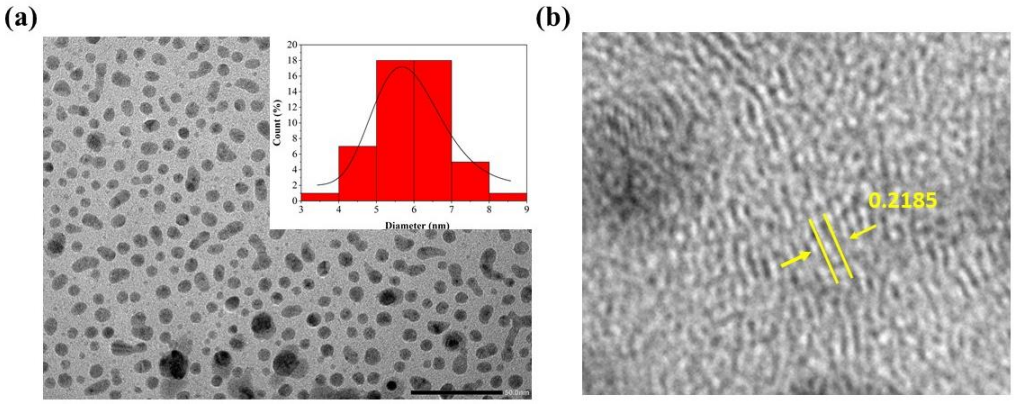

Figure 7. **(a)** TEM image and size distribution histogram (inset); **(b)** HRTEM image of BCU/Ag-CDs.

3.6. pH-responsive carbon dots

The fluorescence intensity of BCU/Ag-CDs under different pH conditions was investigated using a spectrofluorometer. The results, presented in Figure 8a, indicated that the fluorescence intensity of BCU/Ag-CDs was low in acidic conditions but increased significantly in alkaline conditions. Figure 8b shows the emission peaks of BCU/Ag-CDs at an excitation wavelength of 350 nm for different pH values. The findings revealed that as the pH increased from 2 to 13, the fluorescence intensity of BCU/Ag-CDs increased gradually. This phenomenon was attributed to the protonation of the carboxyl groups on the surface of CDs under acidic conditions, leading to non-covalent molecular interactions, such as hydrogen bonds, that caused the aggregation of CDs, and, thus, fluorescence quenching. Moreover, the results indicated that BCU/Ag-CDs remained stable within the pH range of 6 to 9. To explain the aggregation of CDs, the zeta (ζ) potential was used and depicted in Figure 8c. As the pH varied from 2 to 13, the zeta potential exhibited a significant change from 8.15 to -15.17 mV, indicating that the surface functional groups of CDs were deprotonated, resulting in a lesser aggregation of CDs [58].

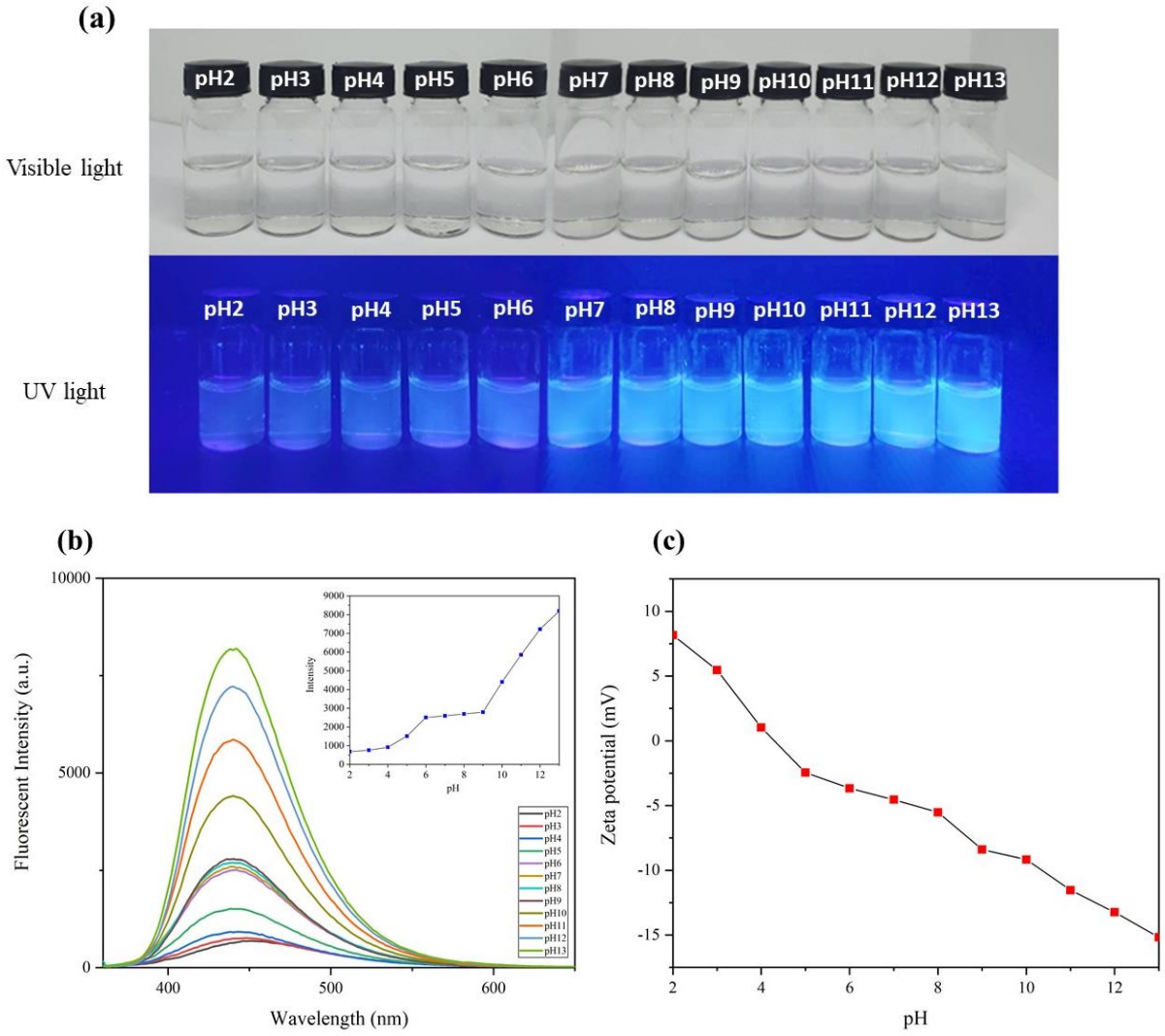

Figure 8. (a) Optical image with pH values ranging from 2-13 under visible and UV light; (b) Fluorescent spectra at 350 nm excitation; (c) Zeta (ζ) potential at pH 2-13 of BCU/Ag-CDs.

4. Conclusions

In summary, boron and silver-doped citric acid/urea-based carbon dots (BCU/Ag-CDs) were synthesized via microwave irradiation in a single step, which was transparent in visible light and exhibited blue fluorescence under UV light. The BCU/Ag-CDs showed the highest quantum yield of 26% among all the synthesized CDs, attributed to their structure's synergistic effect of boron and silver. The BCU/Ag-CDs were spherical with an average size of 5.9 ± 1 nm and well-dispersed. Moreover, the fluorescent intensity of BCU/Ag-CDs was pH-sensitive, showing low emission at acidic pH values and strong emission at alkaline pH values. The findings indicate the potential of these CDs as a material for biomedical applications and sensors.

Funding

This work has received funding support from the National Science, Research, and Innovation Fund (NSRF) and the School of Science, King Mongkut's Institute of Technology Ladkrabang, Thailand (Grant No. RA/TA-2562-M020).

Acknowledgments

The authors would like to thank the Scientific Instruments Center, the School of Science, and King Mongkut's Institute of Technology Ladkrabang.

Conflicts of Interest

The authors declare no conflict of interest.

References

1. El-Shafey.; Asmaa, M. Carbon Dots: Discovery, Structure, Fluorescent Properties, and Applications. *Green Process. Synth.* **2021**, 134-56, https://doi.org/10.1515/gps-2021-0006
2. Jorns, M.; Pappas, D. A Review of Fluorescent Carbon Dots, Their Synthesis, Physical and Chemical Characteristics, and Applications. *Nanomater* **2021**, *11*, 1448, https://doi.org/10.3390/nano11061448
3. Liu, J.; Li, R.; Yang, B. Carbon Dots: A New Type of Carbon-Based Nanomaterial with Wide Applications. *ACS Cent Sci* **2020**, *6*, 2179-95, https://doi.org/10.1021/acscentsci.0c01306.
4. Kang, C.; Huang, Y.; Yang, H.; Yan, X. F.; Chen, Z. P. A Review of Carbon Dots Produced from Biomass Wastes. *Nanomater* **2020,** *10*, 2316, https://doi.org/10.3390/nano10112316.
5. Ang, W. L.; Boon Mee, C. A. L.; Sambudi, N. S.; Mohammad, A. W.; Leo, C. P.; Mahmoudi, E.; Ba-Abbad, M.; Benamor, A. Microwave-Assisted Conversion of Palm Kernel Shell Biomass Waste to Photoluminescent Carbon Dots. *Sci Rep* **2020**, *10*, 21199, https://doi.org/10.1038/s41598-020-78322-1
6. Naik, V.; Zantye, P.; Gunjal, D.; Gore, A.; Anbhule, P.; Kowshik, M.; Bhosale, S. V.; Kolekar, G. Nitrogen-Doped Carbon Dots Via Hydrothermal Synthesis: Naked Eye Fluorescent Sensor for Dopamine and Used for Multicolor Cell Imaging. *ACS Appl Bio Mater* **2019**, *2*, 2069-2077, https://doi.org/10.1021/acsabm.9b00101
7. Kaczmarek, A.; Hoffman, J.; Morgiel, J.; Moscicki, T.; Stobinski, L.; Szymanski, Z.; Malolepszy, A. Luminescent Carbon Dots Synthesized by the Laser Ablation of Graphite in Polyethylenimine and Ethylenediamine. *Mater* **2021**, *14*, 729, https://doi.org/10.3390/ma14040729
8. Chao-Mujica, F. J.; Garcia-Hernández, L.; Camacho-López, S.; Camacho-López, M.; Camacho-López, M. Reyes Contreras, A. D.; Pérez-Rodríguez, A. Carbon Quantum Dots by Submerged Arc Discharge in Water: Synthesis, Characterization, and Mechanism of Formation. *Appl. Phys* **2021**, *129*, https://doi.org/10.1063/5.0040322

9. An, Q.; Lin, Q.; Huang, X.; Zhou, R.; Guo, X.; Xu, W.; Wang, S.; Xu, D.; Chang H. T. Electrochemical synthesis of carbon dots with a Stokes shift of 309 nm for sensing of Fe^{3+} and ascorbic acid. *Dyes Pigm* **2021**, *185*, 108878, https://doi.org/10.1016/j.dyepig.2020.108878
10. Quaid, T.; Ghalandari, V.; & Reza, T. Effect of Synthesis Process, Synthesis Temperature, and Reaction Time on Chemical, Morphological, and Quantum Properties of Carbon Dots Derived from Loblolly Pine. *Biomass* **2022**, *2*, 250-263, https://doi.org/10.3390/biomass2040017
11. Zeng, Q.; Feng, T.; Tao, S.; Zhu, S.; Yang, B. Precursor-Dependent Structural Diversity in Luminescent Carbonized Polymer Dots (CPDs): The Nomenclature. *Light Sci Appl* **2021**, *10*, 142, https://doi.org/10.1038/s41377-021-00579-6
12. Chahal, S.; Yousefi, N.; Tufenkji, N. Green Synthesis of High Quantum Yield Carbon Dots from Phenylalanine and Citric Acid: Role of Stoichiometry and Nitrogen Doping. *ACS Sustain. Chem. Eng* **2020**, *8*, 5566-5575, https://doi.org/10.1021/acssuschemeng.9b07463
13. Uriarte, D.; Domini, C.; Garrido M. New carbon dots based on glycerol and urea and its application in the determination of tetracycline in urine samples. *Talanta* **2019**, *201*, 143-148, https://doi.org/10.1016/j.talanta.2019.04.001
14. Wang, K.; Geng, C.; Wang, F.; Zhao, Y.; Ru, Z. Urea-doped carbon dots as fluorescent switches for the selective detection of iodide ions and their mechanistic study. *RSC Adv* **2021**, *11*, 27645-27652, https://doi.org/10.1039/d1ra04558j
15. Chen, J.; Du, H.; Xu, Y.; Ma, B.; Zheng, Z.; Li, P.; Jiang, Y. A turn-on fluorescent sensor based on coffee-ground carbon dots for the detection of sodium cyclamate. *Mater. Sci.: Mater. Electron* **2021**, *32*, 13581-13587, https://doi.org/10.1007/s10854-021-05933-3
16. Qian, K.; Guo, H.; Chen, G.; Ma, C.; Xing, B. Distribution of different surface modified carbon dots in pumpkin seedlings. *Sci Rep* **2018**, *8*, 7991, https://doi.org/10.1038/s41598-018-26167-0
17. Sahu, S.; Behera, B.; Maiti, T. K.; Mohapatra, S. Simple one-step synthesis of highly luminescent carbon dots from orange juice: application as excellent bio-imaging agents. *ChemComm* **2012**, *48*, 8835-8837, https://doi.org/10.1039/c2cc33796g
18. Xu, D.; Li, Y.; Li, N.; Lei, F.; Liu, J.; Shi, Y.; Yin, L.; Zhang, L. A facile synthesis of CDs from quinoa for nanosensors and bio-imagining. *Nano Express* **2020**, *1*, https://doi.org/10.1088/2632-959X/ab9f53
19. Chahal, S.; Macairan, J. R.; Yousefi, N.; Tufenkji, N.; Naccache, R. Green synthesis of carbon dots and their applications. *RSC Adv* **2021**, *11*, 25354-25363, https://doi.org/10.1039/d1ra04718c
20. Miao, S.; Liang, K.; Zhu, J.; Yang, B.; Zhao, D.; Kong, B. Hetero-atom-doped carbon dots: Doping strategies, properties and applications. *Nano Today* **2020**, *33*, https://doi.org/10.1016/j.nantod.2020.100879
21. Xu, Q.; Kuang, T.; Liu, Y.; Cai, L.; Peng, X.; Sreenivasan Sreeprasad, T.; Zhao, P.; Yu, Z.; Li, N. Heteroatom-doped carbon dots: synthesis, characterization, properties, photoluminescence mechanism and biological applications. *Mater Chem B* **2016**, *4*, 7204-7219, https://doi.org/10.1039/c6tb02131j
22. Kou, X.; Jiang, S.; Park, S. J.; Meng, L. Y. A review: recent advances in preparations and applications of heteroatom-doped carbon quantum dots. *Dalton Trans* **2020**, *49*, 6915-6938, https://doi.org/10.1039/d0dt01004a
23. Li, F.; Yang, D.; Xu, H. Non-Metal-Heteroatom-Doped Carbon Dots: Synthesis and Properties. *Chem* **2019**, *25*, 1165-1176, https://doi.org/10.1002/chem.201802793
24. Kandasamy, G. Recent Advancements in Doped/Co-Doped Carbon Quantum Dots for Multi-Potential Applications. *C* **2019**, *5*, 24, https://doi.org/10.3390/c5020024
25. Nguyen, K. G.; Baragau, I.; Gromicova, R.; Nicolaev, A.; Thomson, S. A.; Rennie, A.; Power, N. P.; Sajjad, M. T.; Kellici, S. Investigating the effect of N-doping on carbon quantum dots structure, optical properties and metal ion screening. *Sci. Rep* **2022**, *12*, 13806, https://doi.org/10.1038/s41598-022-16893-x
26. Tian, B.; Fu, T.; Wan, Y.; Ma, Y.; Wang, Y.; Feng, Z.; Jiang, Z. B-and N-doped carbon dots by one-step microwave hydrothermal synthesis: tracking yeast status and imaging mechanism. *Nanobiotechnology* **2021**, *19*, 1-12, https://doi.org/10.1186/s12951-021-01211-w
27. Lan, J.; Zheng, X. H.; Song, L. L.; Wang, R. N.; Zeng, Z. B, C and N adatoms effects on the transport properties in zigzag graphene nanoribbons. *Solid State Commun* **2012**, *152*, 1635-1640, https://doi.org/10.1016/j.ssc.2012.04.074
28. Tomskaya, A. E.; Prosvirin, I. P.; Egorova, M. N.; Smagulova, S. A.; Asanov, I. P. Structural and Optical Properties of N-Doped and B-Doped Carbon Dots. *Struct Chem* **2020**, *61*, 818-825, https://doi.org/10.1134/s0022476620050194

29. Liu, H.; Liu, Z.; Zhang, J,; Zhi, L.; Wu, M. Boron and nitrogen co-doped carbon dots for boosting electrocatalytic oxygen reduction. *New Carbon Mater*, **2021**, *36*, 585-593, https://doi.org/10.1016/s1872-5805(21)60043-4
30. Xu, J.; Guo, Y.; Gong, T.; Cui, K.; Hou, L.; Yuan, C. B, N co-doped carbon dots based fluorescent test paper and hydrogel for visual and efficient dual ion detection. *Inorg. Chem. Commun* **2022**, *145*, 110047, https://doi.org/10.1016/S1872-5805(21)60043-4
31. Atabaev, T. S. Doped Carbon Dots for Sensing and Bioimaging Applications: A Minireview. *Nanomater* **2018**, *8*, 342, https://doi.org/10.3390/nano8050342
32. Lin, L.; Luo, Y.; Tsai, P.; Wang, J.; Chen, X. Metal ions doped carbon quantum dots: Synthesis, physicochemical properties, and their applications. *TrAC* **2018**, *103*, 87-101, https://doi.org/10.1016/j.trac.2018.03.015
33. Tejwan, N.; Saini, A. K.; Sharma, A.; Singh, T. A.; Kumar, N.; Das, J. Metal-doped and hybrid carbon dots: A comprehensive review on their synthesis and biomedical applications. *CR*, **2021**, *330*, 132-150, https://doi.org/10.1016/j.jconrel.2020.12.023
34. Wang, J.; Zhu, Y.; Xie, X.; He, X.; Fan, J.; Chen, A. Effect of ultra-trace Ag doping on the antibacterial performance of carbon quantum dots. *Environ. Chem. Eng* **2022**, *10*, 107112, https://doi.org/10.1016/j.jece.2021.107112
35. Gunjal, D. B.; Nille, O. S.; Naik, V. M.; Shejwal, R. V.; Kolekar, G. B.; Gore, A. H. Heteroatom/metal ion-doped carbon dots for sensing applications. *Anal. Chem* **2023**, 181-197, https://doi.org/10.1016/B978-0-323-98350-1.00002-5
36. Xu, Q.; Su, R.; Chen, Y.; Theruvakkattil Sreenivasan, S.; Li, N.; Zheng, X.; Zhu, J.; Pan, H.; Li, W.; Xu, C. Metal charge transfer doped carbon dots with reversibly switchable, ultra-high quantum yield photoluminescence. *ACS Appl. Nano Mater* **2018**, *1*, 1886-1893, https://doi.org/10.1021/acsanm.8b00277
37. Rub Pakkath, S. A.; Chetty, S. S.; Selvarasu, P.; Vadivel Murugan, A.; Kumar, Y.; Periyasamy, L.; Santhakumar, M.; Sadras, S. R.; Santhakumar, K. Transition metal ion (Mn^{2+}, Fe^{2+}, Co^{2+}, and Ni^{2+})-doped carbon dots synthesized via microwave-assisted pyrolysis: a potential nanoprobe for magneto-fluorescent dual-modality bioimaging. *ACS Biomater. Sci. Eng* **2018**, *4*, 2582-2596., https://doi.org/10.1021/acsbiomaterials.7b00943.
38. Dang, D. K.; Pham, T. T. Metal Ions Doped-Carbon Dots: Synthetic Approaches, Physicochemical Properties and Their Applications." Journal of *Res. Sci. Technol. Educ* **2022**, *73*, 54-63, https://doi.org/10.1021/acsbiomaterials.7b00943
39. Niu, Q.; Gao, K.; Lin, Z.; Wu, W. Amine-capped carbon dots as a nanosensor for sensitive and selective detection of picric acid in aqueous solution via electrostatic interaction. *Anal. Methods* **2013**, *5*, 6228-6233, https://doi.org/10.1039/C3AY41275J
40. Bourlinos, A. B.; Trivizas, G.; Karakassides, M. A.; Baikousi, M.; Kouloumpis, A.; Gournis, D.; Bakandritsos, A.; Hola, K.; Kozak, O.; Zboril, R. Green and simple route toward boron doped carbon dots with significantly enhanced non-linear optical properties. *C* **2015**, *83*, 173-179, https://doi.org/10.1016/j.carbon.2014.11.032
41. Omidi, M.; Yadegari, A.; Tayebi, L. Wound dressing application of pH-sensitive carbon dots/chitosan hydrogel. *RSC adv*, **2017**, *7*, 10638-10649, https://doi.org/10.1039/C6RA25340G
42. Balakrishnan, T.; Ang, W. L.; Mahmoudi, E.; Mohammad, A. W.; Sambudi, N. S. Formation mechanism and application potential of carbon dots synthesized from palm kernel shell via microwave assisted method. *CRC* **2022**, *5*, 150-166, https://doi.org/10.1016/j.crcon.2022.01.003
43. So, R. C.; Sanggo, J. E.; Jin, L.; Diaz, J. M. A.; Guerrero, R. A.; He, J. Gram-scale synthesis and kinetic study of bright carbon dots from citric acid and Citrus japonica via a microwave-assisted method. *ACS omega* **2017**, *2*, 5196-5208., https://doi.org/10.1021/acsomega.7b00551
44. Liu, Y.; Li, W.; Wu, P.; Ma, C.; Wu, X.; Xu, M.; Luo, S.; Xu, Z.; Liu, S. Hydrothermal synthesis of nitrogen and boron co-doped carbon quantum dots for application in acetone and dopamine sensors and multicolor cellular imaging. *Sens. Actuators B Chem*, **2019**, *281*, 34-43, https://doi.org/10.1016/j.snb.2018.10.075
45. Tian, B.; Fu, T.; Wan, Y.; Ma, Y.; Wang, Y.; Feng, Z.; Jiang, Z. B-and N-doped carbon dots by one-step microwave hydrothermal synthesis: tracking yeast status and imaging mechanism. *Journal of Nanobiotechnology* **2021**, *19*, 1-12, https://doi.org/10.1186/s12951-021-01211-w
46. Mohammed, L. J.; Omer, K. M. Dual functional highly luminescence B, N Co-doped carbon nanodots as nanothermometer and Fe^{3+}/Fe^{2+} sensor. *Sci. Rep* **2020**, *10*, 3028, https://doi.org/10.1038/s41598-020-59958-5

47. Wang, H.; Sun, P.; Cong, S.; Wu, J.; Gao, L.; Wang, Y.; Dai, X.; Yi, Q.; Zou, G. Nitrogen-doped carbon dots for "green" quantum dot solar cells. *Nanoscale Res. Lett* **2016**, *11*, 1-6, https://doi.org/10.1186/s11671-016-1231-1
48. Ye, Q.; Yan, F.; Shi, D.; Zheng, T.; Wang, Y.; Zhou, X.; Chen, L. N, B-doped carbon dots as a sensitive fluorescence probe for Hg^{2+} ions and 2, 4, 6-trinitrophenol detection for bioimaging. *Photochem. Photobiol. B, Biol* **2016**, *162*, 1-13, https://doi.org/10.1016/j.jphotobiol.2016.06.021
49. Shi, L.; Zhu, C.; He, H.; Zhu, D.; Zhang, Z.; Pang, D.; Tian, Z. Near-infrared Ag_2Se quantum dots with distinct absorption features and high fluorescence quantum yields. *RSC adv* **2016**, *6*, 38183-38186, https://pubs.rsc.org/en/content/articlelanding/2016/ra/c6ra04987g.
50. Sharma, R.; Dhillon, A.; Kumar, D. Mentha-stabilized silver nanoparticles for high-performance colorimetric detection of Al (III) in aqueous systems. *Sci. Rep* **2018**, *8*, 5189, https://doi.org/10.1038/s41598-018-23469-1
51. Mohamedkhair, A. K.; Drmosh, Q.; Yamani, Z. H. Silver nanoparticle-decorated tin oxide thin films: synthesis, characterization, and hydrogen gas sensing. *Front. Mater* **2019**, *6*, 188, https://doi.org/10.3389/fmats.2019.00188
52. Emam, A.; Loutfy, S. A.; Mostafa, A. A.; Awad, H.; Mohamed, M. B. Cyto-toxicity, biocompatibility and cellular response of carbon dots–plasmonic based nano-hybrids for bioimaging. *RSC adv* **2017**, *7*, 23502-23514, https://doi.org/10.1039/C7RA01423F
53. Liu, M. Optical properties of carbon dots: a review. *Nanoarchitectonics* **2020**, 1-12, https://doi.org/10.37256/nat.112020124.1-12
54. Dutta, A.; Dutta. R. R.; Gogoi, S. Optical properties of carbon dots and their applications. Carbon Dots in Agricultural Systems, *Elsevier* **2022**, 135-153, https://doi.org/10.1016/B978-0-323-90260-1.00003-6
55. Van Nguyen, C.; Lee, S.; Chung, Y. G.; Chiang, W.; Wu, K. C. Synergistic effect of metal-organic framework-derived boron and nitrogen heteroatom-doped three-dimensional porous carbons for precious-metal-free catalytic reduction of nitroarenes. *Appl. Catal. B: Environ* **2019**, *257*, 117888, https://doi.org/10.1016/j.apcatb.2019.117888
56. Zhuo, S. J.; Fang, J.; Wang, J.; Zhu, C. Q. One-step hydrothermal synthesis of silver-doped carbon quantum dots for highly selective detection of uric acid. *Methods Appl. Fluoresc* **2019**, *8*, 015005, https://doi.org/10.1088/2050-6120/ab5d8c
57. Yang, Y. Z.; Xiao, N.; Liu, S. G.; Han, L.; Li, N. B.; Luo, H. Q. pH-induced aggregation of hydrophilic carbon dots for fluorescence detection of acidic amino acid and intracellular pH imaging. *Mater Sci and Eng* **2020**, *108*, 110401, https://doi.org/10.1016/j.msec.2019.110401
58. Bayati, M.; Dai, J.; Zambrana, A.; Rees, C.; Cortalezzi, M. F. Effect of water chemistry on the aggregation and photoluminescence behavior of carbon dots. *Journal of Environ Sci* **2018**, *65*, 223-235, https://doi.org/10.1016/j.jes.2017.03.009